Evidence for Cerebrospinal Fluid Entry Into the Optic Nerve via a Glymphatic Pathway

Emily Mathieu,[1–3] Neeru Gupta,[1–4] Amir Ahari,[1] Xun Zhou,[1,2] Joseph Hanna,[1–3] and Yeni H. Yücel[1–3]

[1]Keenan Research Centre for Biomedical Science, Li Ka Shing Knowledge Institute, St. Michael's Hospital, Toronto, Ontario, Canada
[2]Department of Ophthalmology and Vision Sciences, St. Michael's Hospital, University of Toronto, Toronto, Ontario, Canada
[3]Department of Laboratory Medicine and Pathobiology, St. Michael's Hospital, University of Toronto, Toronto, Ontario, Canada
[4]Glaucoma Unit, St. Michael's Hospital, Toronto, Ontario, Canada

Correspondence: Yeni H. Yücel, Keenan Research Centre for Biomedical Science, St. Michael's Hospital, 30 Bond Street, 209 LKSKI Room 409, Toronto, Ontario M5B 1W8, Canada; yucely@smh.ca.

Submitted: May 24, 2017
Accepted: August 17, 2017

Citation: Mathieu E, Gupta N, Ahari A, Zhou X, Hanna J, Yücel YH. Evidence for cerebrospinal fluid entry into the optic nerve via a glymphatic pathway. *Invest Ophthalmol Vis Sci*. 2017;58:4784–4791. DOI:10.1167/iovs.17-22290

Purpose. The purpose of this study was to determine whether cerebrospinal fluid (CSF) enters the optic nerve via a glymphatic pathway and whether this entry is size-dependent.

Methods. Fluorescent dextran tracers (fluorescein isothiocyanate [FITC]) of four different sizes (10, 40, 70, and 500 kDa) and FITC-ovalbumin (45 kDa) were injected into the CSF of 15 adult mice. Tracer distribution in the orbital optic nerve at 1 hour after injection was assessed in tissue sections with confocal microscopy. Tracer distribution within the optic nerve was studied in relation to blood vessels and astrocytes identified by isolectin histochemistry and glial fibrillary acidic protein (GFAP) immunofluorescence, respectively. Aquaporin 4 (AQP4) immunostaining was performed to assess astrocytic endfeet in relation to CSF tracer.

Results. One hour following tracer injection into CSF, all tracer sizes (10–500 kDa) were noted in the subarachnoid space surrounding the orbital optic nerve. In all cases, 10 kDa ($n = 4/4$) and 40 kDa ($n = 3/3$) tracers were noted within the optic nerve, while 70-kDa tracer was occasionally noted ($n = 1/4$). Tracer found within the nerve was specifically localized between isolectin-labeled blood vessels and GFAP-positive astrocytes or AQP4-labeled astrocytic endfeet. The 500-kDa tracer was not detected within the optic nerve.

Conclusions. To our knowledge, this is the first evidence of a glymphatic pathway in the optic nerve. CSF enters the optic nerve via spaces surrounding blood vessels, bordered by astrocytic endfeet. CSF entry into paravascular spaces of the optic nerve is size-dependent, and this pathway may be highly relevant to optic nerve diseases, including glaucoma.

Keywords: glymphatic, paravascular, perivascular, optic nerve, cerebrospinal fluid, glaucoma

Cerebrospinal fluid (CSF) surrounds the central nervous system to provide buoyancy, nutrient delivery, and a pathway for clearance of metabolic waste.[1] The optic nerve is surrounded by CSF within the subarachnoid space, though what role, if any, CSF plays in optic nerve development, health, and disease is poorly understood. CSF may be a potential source of beneficial proteins and peptides such as neurotrophins and growth factors.[2–4] Also, the relationship between the CSF, eye, and optic nerve is presently of great interest for our understanding of the pathogenesis of glaucoma. CSF pressure[5–7] and flow/turnover[8,9] have both been linked to progression of this irreversible blinding disease.

Few studies have investigated whether CSF and its molecular components enter into the optic nerve, although CSF-injected tracer has been noted in the optic nerve in passing.[10–12] In the brain, a glymphatic pathway has been described in which CSF flows into and out of the parenchyma along spaces formed between blood vessels and an ensheathing layer of astrocytic endfeet.[13,14] The glymphatic pathway consists of paravascular inflow of CSF into brain parenchyma and clearance of fluid and extracellular solutes from the interstitium. The brain's glymphatic system clears harmful metabolites, facilitated by aquaporin 4 (AQP4) water channels on astrocytic endfeet.[14] It is not known whether a similar paravascular pathway also facilitates entry of CSF into the optic nerve.

The mouse has CSF pressure,[15] drainage pathways,[16] and optic nerve anatomy[17] similar to humans. The ready availability of transgenic mice and established optic neuropathy models makes this an attractive candidate for clinically relevant eye studies. Here we aim to characterize CSF entry into the mouse optic nerve, including the microanatomical route and size-exclusion properties.

Methods

Experimental Animals

Albino mice ($n = 19$, 11 female/8 male; CD1; Charles River, Senneville, QC, Canada) weighing between 25 and 40 g were housed on a 12-hour light-dark cycle and fed standard food ad libitum. All experimental protocols adhered to the ARVO Statement for the Use of Animals in Ophthalmic and Vision Research and were approved by the institutional animal care committee.

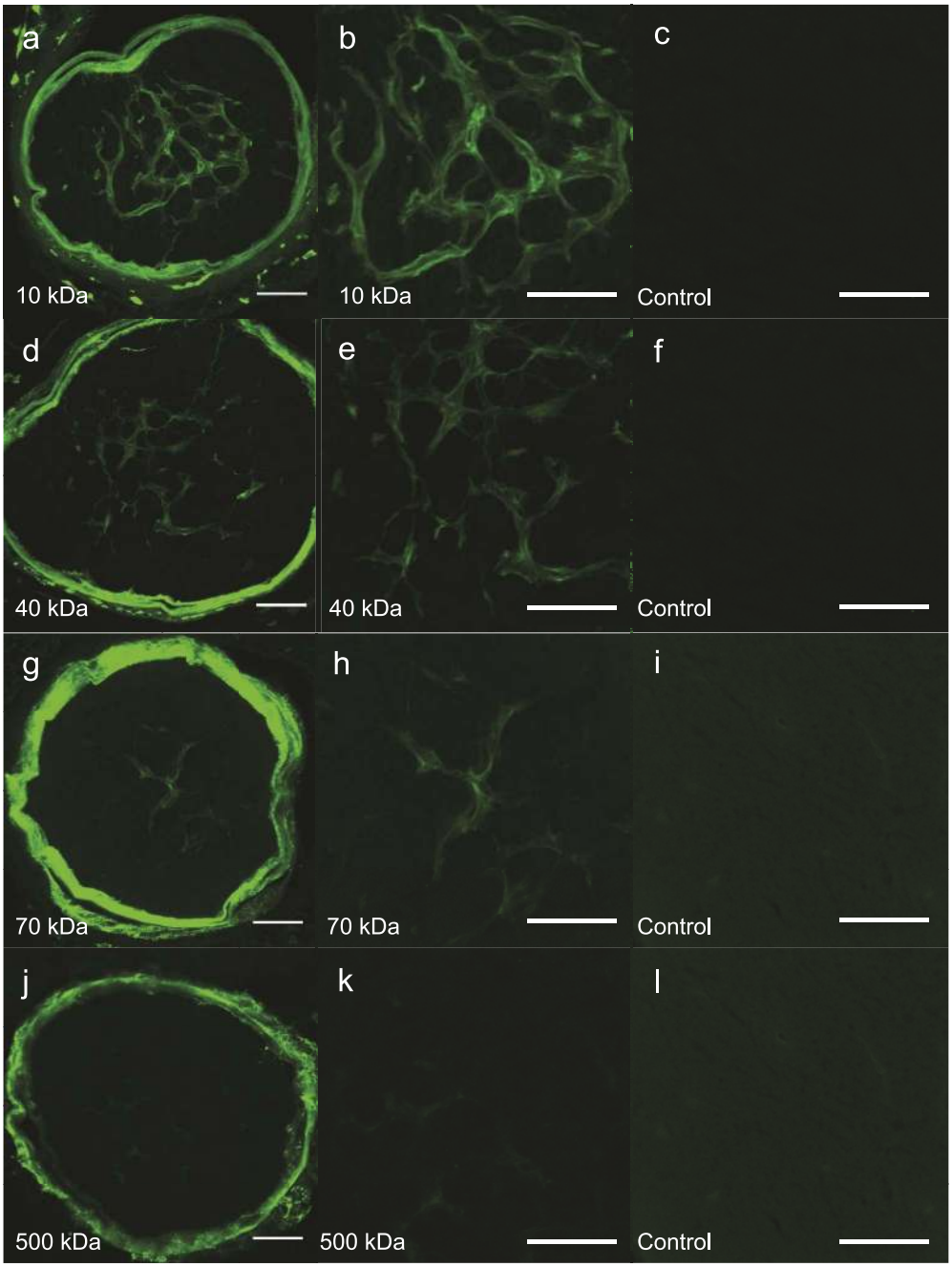

Figure 1. Optic nerve cross sections following CSF injection of various-sized tracers: 10 kDa (**a**, **b**), 40 kDa (**d**, **e**), 70 kDa (**g**, **h**), and 500 kDa (**j**, **k**). All optic nerves showed CSF (*green*) surrounding the optic nerve in the subarachnoid space (**a**, **d**, **g**, **j**). At higher power (**b**, **e**, **h**, **k**), smaller tracers (≤70 kDa) were seen within the optic nerve in branching tubular networks. Minimal to no signal was observed in controls (**c**, **f**, **i**, **l**). *Scale bars*: 50 μm.

Fluorescent Tracers

Lysine-fixable fluorescein isothiocyanate (FITC) conjugated to various sizes of dextran (10, 40, 70, and 500 kDa (Invitrogen, Carlsbad, CA, USA) and to ovalbumin (45 kDa; Invitrogen) was used as a tracer in these experiments. All FITC conjugates were reconstituted in PBS to final concentrations of 25 mg/mL (10, 40, and 70 kDa) or 10 mg/mL (500 kDa, ovalbumin). The degree of labeling (moles of dye per mole of dextran) increased with increasing tracer size, allowing similar fluorescence levels for all tracers.

Fluorescent Tracer Injection Into CSF

Under general anesthesia (isoflurane, 2% in O_2), mice were mounted on a stereotaxic frame (Kopf Instruments, Tujunga, CA, USA). The cisterna magna was exposed by making a dorsal skin incision from the base of the neck to the tip of the occiput and bluntly dissecting the muscles of the neck. Using a 33-gauge needle (Hamilton Company, Reno, NV) and a 10-μL Hamilton syringe, 3 μL of tracer was injected into the cisterna magna as a slow bolus over the course of 1 to 2 minutes. It was previously shown that this injection technique does not increase intracranial pressure.[18] The number of animals

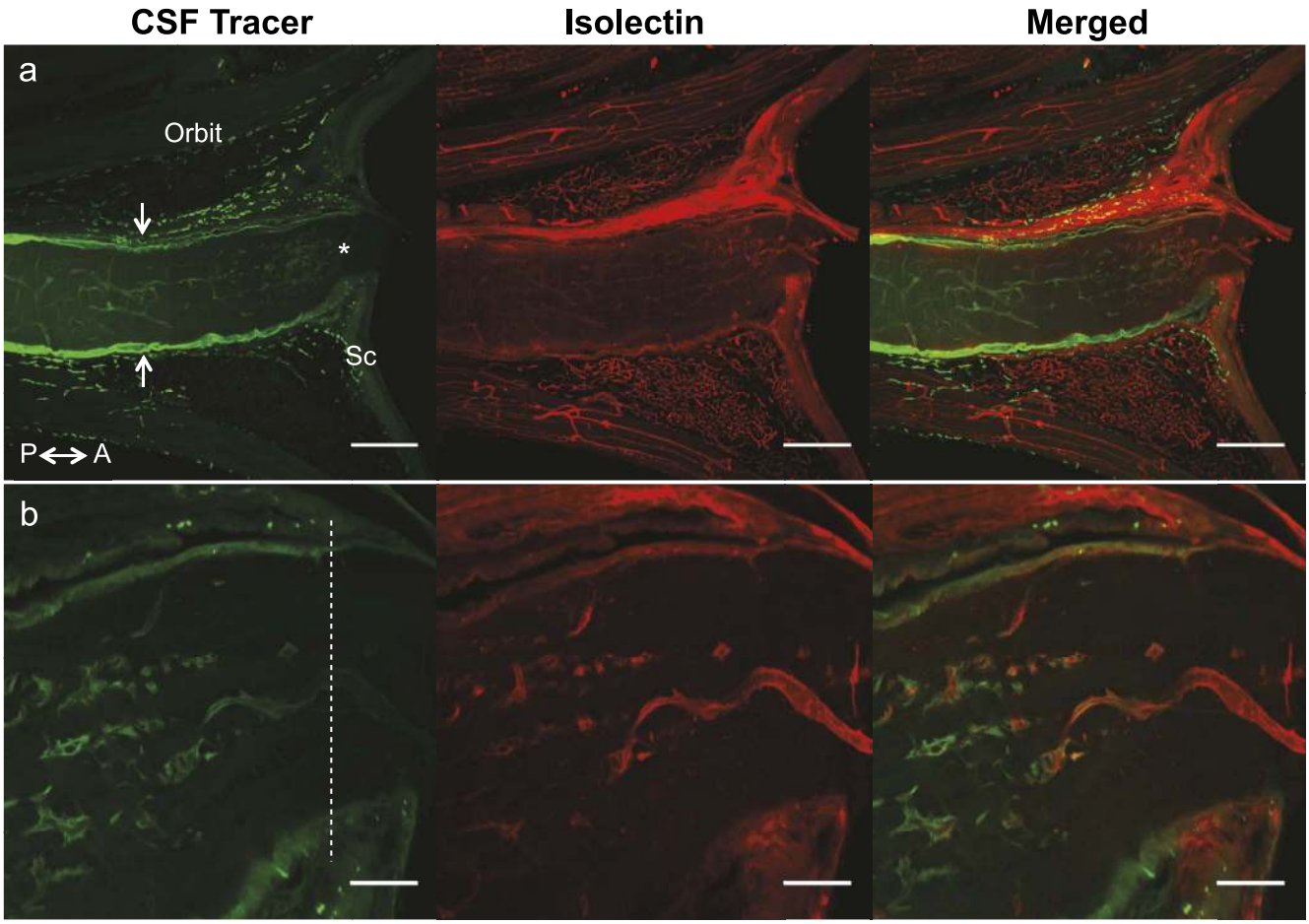

FIGURE 2. Sagittal optic nerve after tracer injection into CSF. (**a**) CSF tracer (10 kDa; *green*) lines the optic nerve within the subarachnoid space (*arrows*) and is also seen inside the nerve forming a branching network spanning the length of the nerve. Signal intensity decreases anteriorly up to the glia lamina (*asterisk*). Isolectin-labeled blood vessels are seen in *red*. (**b**) CSF in the nerve was observed up to the posterior sclera/glia lamina (*dotted line*). Sc, sclera; P, posterior; A, anterior. *Scale bars*: (**a**) 200 μm, (**b**) 50 μm.

injected with each tracer size was as follows: 10 kDa ($n = 4$), 40 kDa ($n = 4$), 70 kDa ($n = 5$), 500 kDa ($n = 4$), ovalbumin ($n = 1$). Mice were kept in a warm chamber under isoflurane anesthesia for the remainder of the experiment.

Euthanasia and Tissue Preparation

Approximately 10 minutes prior to euthanasia, mice were given intraperitoneal ketamine/xylazine (200 and 10 mg/kg, respectively) in preparation for the perfusion procedure. One hour after tracer injection, mice were euthanized by intracardiac perfusion with cold saline, followed by 2% paraformaldehyde (Electron Microscopy Sciences, Hatfield, PA, USA). Control mice ($n = 2$) were euthanized using the same procedure without tracer injection.

Whole heads were harvested and postfixed overnight in 2% paraformaldehyde (Electron Microscopy Sciences, Hatfield, PA, USA) at 4°C followed by cryoprotection in 10% sucrose solution for 1 day and 20% sucrose for 2 days. Intraorbital optic nerves with surrounding orbital tissue were isolated and snap-frozen in isopentane cooled by dry ice before embedding in cryomatrix (Shandon Cryomatrix; Thermo Scientific, Kalamazoo, MI, USA). Left optic nerves were coronally sectioned and right optic nerves were sagittally sectioned (30 μm) with a cryostat (CM 1900; Leica, Nussloch, Germany).

Analysis of Tracer Fluorescence in Optic Nerve Sections

From all mice, multiple coronal optic nerve sections located between the sclera and 500 μm behind the globe were evaluated. After rinsing with PBS and mounting with antifade mounting medium (Fluorescence Mounting Medium; Dako, Burlington, ON, Canada), confocal imaging (LSM 700; Zeiss, Oberkochen, Germany) was performed to identify and map tracer distribution within the nerve. Detection of tracer in the subarachnoid space surrounding the intraorbital optic nerve was defined as a successful injection and resulted in the following final sample sizes: 10 kDa ($n = 4$), 40 kDa ($n = 3$), 70 kDa ($n = 4$), 500 kDa ($n = 3$), and ovalbumin ($n = 1$). All sections were imaged alongside noninjected control sections to account for background tissue autofluorescence.

Histochemistry and Immunofluorescence

Isolectin B4 stain was used to label blood vessel endothelium in optic nerve tissue sections of mice euthanized 1 hour after tracer injection into CSF. Coronal and sagittal sections were rinsed (3 × 5 minutes in PBS) and stained overnight at 4°C with isolectin B4 from *Griffonia simplicifolia* conjugated to Alexa Fluor 647 (Invitrogen) diluted 1:50 from a 1 mg/mL stock solution in 0.3% Triton X-100 PBS solution.

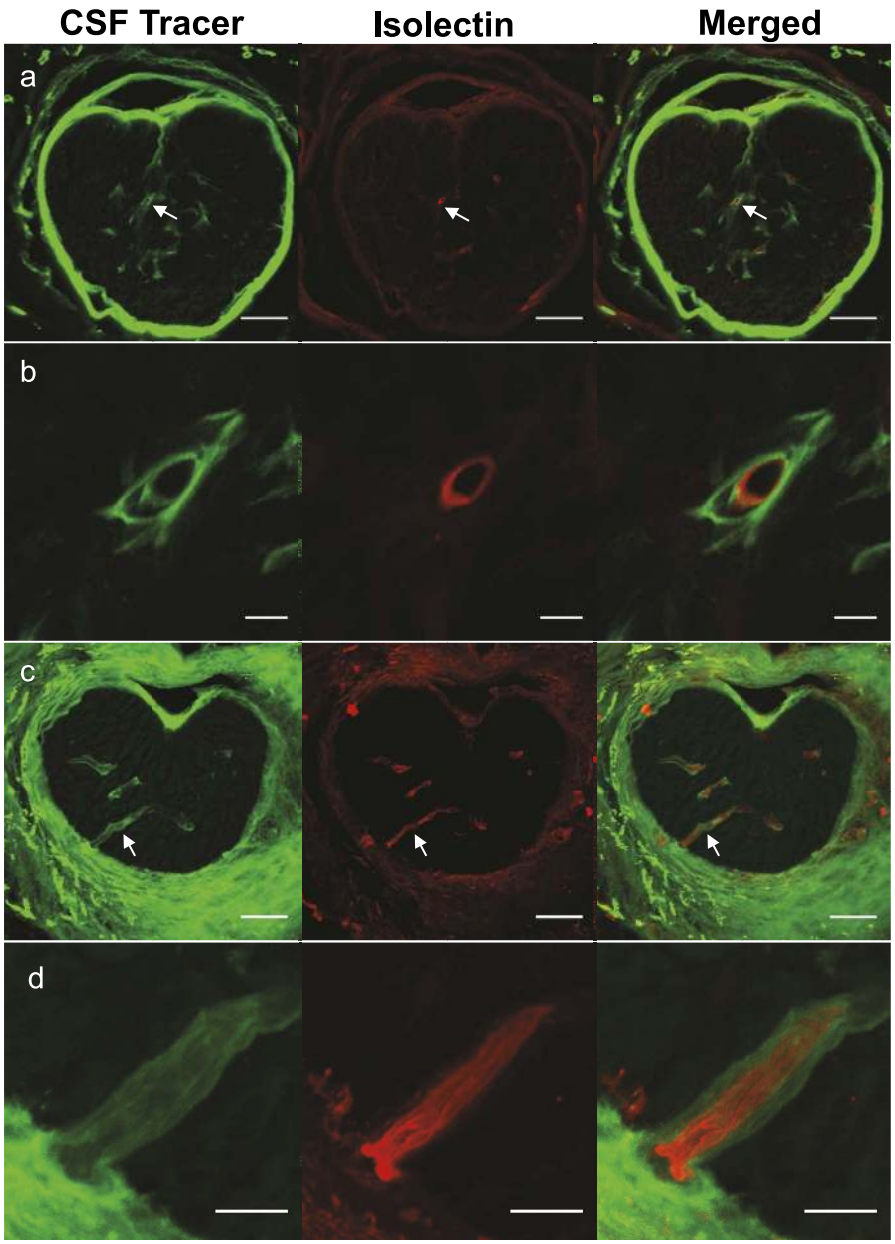

FIGURE 3. (**a**, **c**) Optic nerve cross sections show CSF tracer (10 kDa; *green*) in the subarachnoid space and inside the nerve surrounding several isolectin-labeled blood vessels (*red*) (*arrows*). (**b**) High magnification shows blood vessel in *red* surrounded by CSF. (**d**) A sagittal profile of the vessel in (**c**) shows a sleeve of CSF surrounding the blood vessel arising from the subarachnoid space. *Scale bars*: (**a**) 50 μm, (**b**) 5 μm, (**c**) 50 μm, (**d**) 10 μm.

To label astrocytes, coronal sections were rinsed and blocked with goat serum (2% in PBS with 0.5% Triton X-100; Sigma-Aldrich Corp, St. Louis, MO, USA) for 40 minutes at room temperature. Incubation with rabbit anti–glial fibrillary acidic protein (anti-GFAP) primary antibody (1:200; Invitrogen) overnight at 4°C was followed by secondary antibody incubation for 2 hours at room temperature (goat anti-rabbit conjugated to Alexa Fluor 647, 1:500; Invitrogen).

To label astrocytic endfeet, AQP4 immunofluorescence staining of coronal sections was performed. After blocking with goat serum (5% in PBS with 0.5% Triton X-100) for 40 minutes, sections were incubated overnight at 4°C with rabbit anti-rat AQP4 primary antibody (1:200; Chemicon, EMD Millipore, Billerica, MA, USA), followed by secondary antibody (goat anti-rabbit Alexa Fluor 555, 1:500; Invitrogen) for 2 hours at room temperature. AQP4 staining was conducted on sections after CSF injections of FITC-dextran 10-kDa, FITC-dextran 40-kDa, and FITC-ovalbumin 45-kDa tracers.

All antibodies were diluted in their respective blocking buffers, and tissues were rinsed three times for 5 minutes between all steps, except after blocking. Negative controls were obtained by omitting the primary antibody.

Confocal Microscopy of Optic Nerve Sections

Confocal images were taken using 20× (air) and 63× (oil) objective lenses. Lasers used for excitation included 488 nm (FITC), 555 nm (Alexa Fluor 555), and 639 nm (Alexa Fluor 647). Laser power was set to 2.0% for all imaging. Pinhole size for the FITC channel was consistently 1.0 Airy units and variable for Alexa Fluor 555 and 647. Gain settings for FITC imaging were in the range of 550 to 700 V. Detection

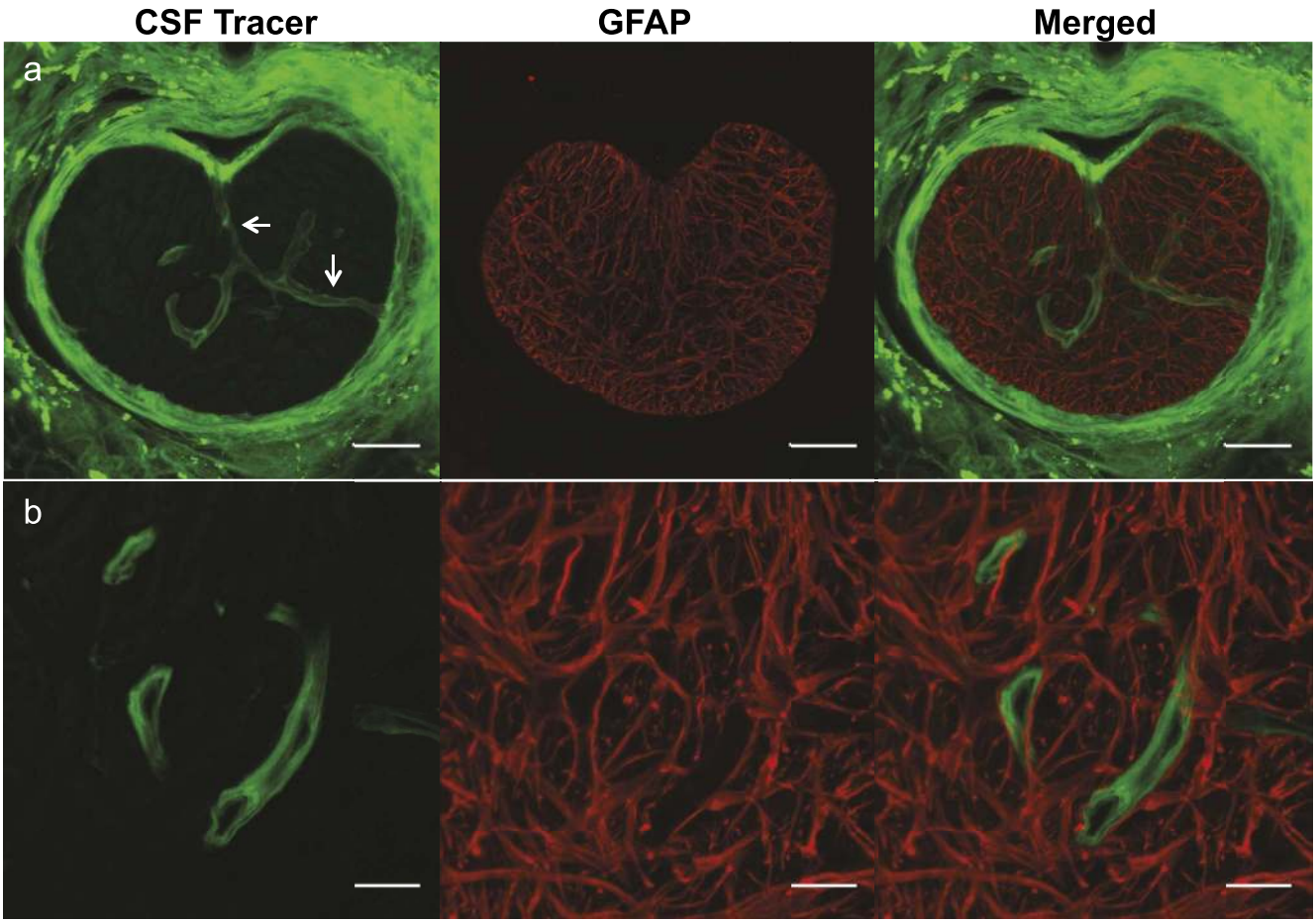

FIGURE 4. (**a**) CSF tracer panel shows an optic nerve cross section with tracer (10 kDa; *green*) in the surrounding subarachnoid space and in a branching network within the nerve. A continuous channel of CSF tracer (*arrows*) spans the nerve between two regions of subarachnoid space. GFAP panel shows labeled astrocytes (*red*) forming a network throughout the cross section of the nerve. (**b**) Higher magnification shows CSF in the nerve is bordered by astrocytes in the merged panel. *Scale bars*: (**a**) 50 μm, (**b**) 15 μm.

wavelength ranges were 493 to 800 nm for FITC only, 300 to 550 and 560 to 800 nm for simultaneous FITC and Alexa Fluor 555 imaging, and 300 to 629 and 644 to 800 nm for simultaneous FITC and Alexa Fluor 647 imaging. For optic nerve cross section imaging of FITC-dextran, 15-μm-thick Z-stacks were collected with a 0.9-μm step size. Z-stacks were processed using ImageJ (Fiji; version 2.0.0-rc-54/1.51g) image-processing software (http://imagej.nih.gov/ij/; provided in the public domain by the National Institutes of Health, Bethesda, MD, USA) to create maximum intensity projections and color composites. Sections were analyzed to determine the location of tracer in relation to labeled blood vessels and astrocytes.

RESULTS

CSF Entry Into Optic Nerve

One hour following tracer injection into CSF, all FITC-dextran sizes were present in the subarachnoid space surrounding the intraorbital optic nerve ($n = 14/14$). In 10-kDa ($n = 4/4$; Figs. 1a, 1b) and 40-kDa ($n = 3/3$; Figs. 1d, 1e) trials, intense tracer fluorescence was detected within the optic nerve. Tracer within the nerve appeared in a network of branching tubular formations spanning the cross section of the nerve (Figs. 1a, 1b, 1d, 1e). Tracer fluorescence was clearly distinguishable from background autofluorescence seen in noninjected controls imaged using the same parameters (Figs. 1c, 1f). Using higher sensitivity acquisition settings, minimal tracer fluorescence was detected in the optic nerve in one 70-kDa trial ($n = 1/4$; Figs. 1g, 1h), while 500-kDa tracers were not seen in the nerve (Figs. 1j, 1k). Figures 1i and 1l depict background autofluorescence for 70- and 500-kDa images. Sagittal sections of optic nerve showed a continuous network of tracer along the length of the nerve with a decreasing intensity anteriorly (Fig. 2). Tracer was not detected beyond the level of the sclera/glia lamina (Fig. 2b).

Paravascular Distribution of CSF-Injected Tracer in Optic Nerve

CSF-injected tracer was seen surrounding isolectin-labeled blood vessels in the optic nerve, both in direct contact with blood vessel endothelium and also approximately 1 to 2 μm peripheral to the endothelium (Fig. 3). Tracer was also observed surrounding blood vessels entering the optic nerve from the subarachnoid space (Figs. 3c, 3d). GFAP immunohistochemistry showed abundant astrocyte straining throughout the nerve (Fig. 4). Channels of paravascular tracer infiltrating the nerve from the subarachnoid space were externally bordered by GFAP-positive astrocytes (Fig. 4). Within the nerve, AQP4 staining showed astrocytic endfeet immediately adjacent to CSF tracers (Figs. 5, 6). AQP4 partially overlapped with CSF tracer (Fig. 6).

Investigative Ophthalmology & Visual Science

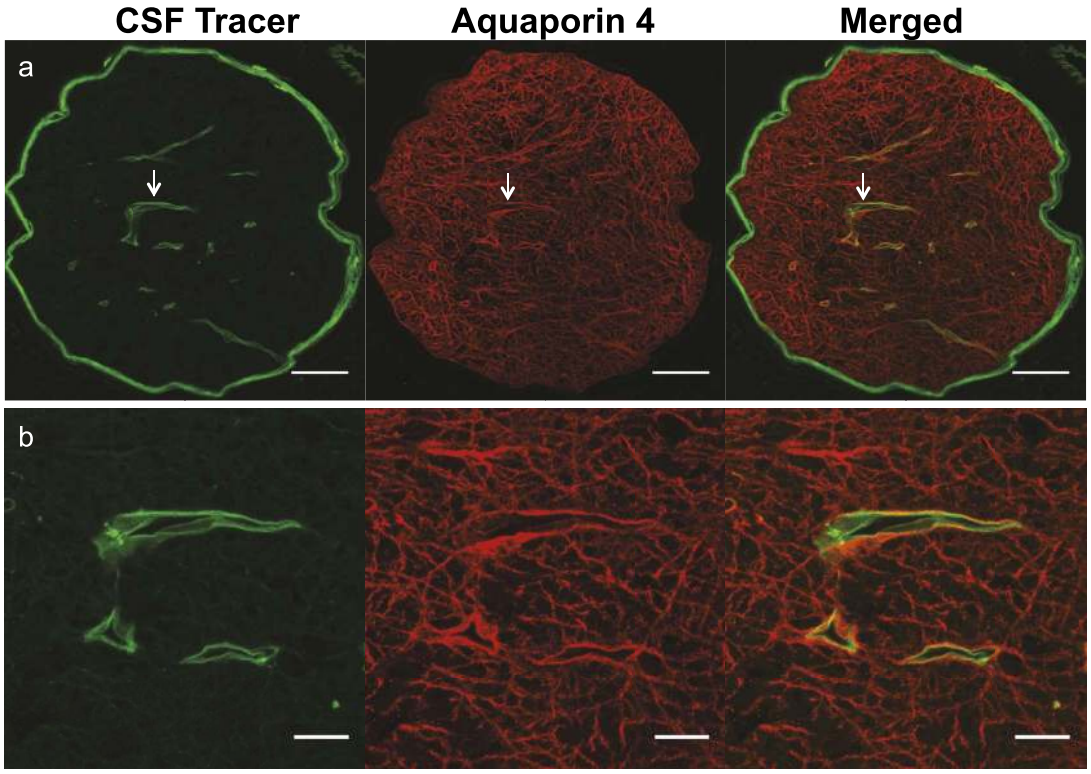

FIGURE 5. (**a**) CSF tracer panel shows optic nerve cross section with CSF tracer (ovalbumin; *green*) in the surrounding subarachnoid space. Within the nerve, distinct channels of CSF tracer (*arrows*) are lined by AQP4 immunoreactivity (*red*) in the merged image. (**b**) Higher magnification shows aquaporin-labeled astrocytic endfeet immediately adjacent to CSF tracer in the nerve. *Scale bars*: (**a**) 50 μm, (**b**) 15 μm.

DISCUSSION

This study provides the first evidence of CSF entry via paravascular spaces into the orbital optic nerve. These findings build on early work in which tracers injected into the CSF were noted in the optic nerve.[10–12] Previously, diaminoacridine dyes[11] (469 Da), sodium fluorescein[10] (376 Da), or horseradish peroxidase[12] (44 kDa) were injected into CSF and found diffusely throughout the optic nerve. These studies were conducted in rabbit,[11] cat,[11] dog,[11] guinea pig,[11] rhesus monkey,[10,11] and mouse.[12] The route of entry was either not described[11] or assumed to be free diffusion from the

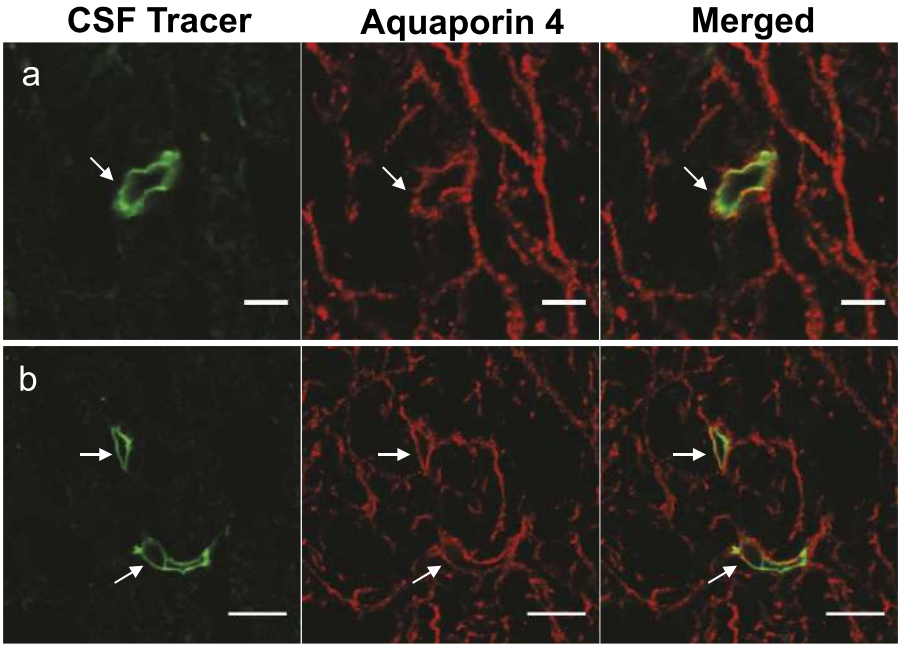

FIGURE 6. (**a**, **b**) Single z-plane confocal cross sections of channels (*arrows)* of CSF tracer (10 kDa dextran; *green*) in the optic nerve ensheathed in AQP4-labeled astrocytic endfeet (*red*). Merged images show AQP4 partially overlaps with CSF tracer. *Scale bars*: (**a**) 5 μm, (**b**) 10 μm.

subarachnoid space.[10,12] A recent postmortem study in which India ink was injected into the subarachnoid space of human optic nerves showed tracer surrounding blood vessels; however, the authors acknowledged dificulty interpreting these results due to tracer injection into postmortem tissue and sample size of two.[19] Our findings indicate that CSF enters the optic nerve, with a number of potential implications for optic nerve pathologies.

This is also the first time, to our knowledge, that variable-size entry of molecules from the CSF into the optic nerve has been described. Our findings show an approximate size cut-off of 70 kDa for molecules entering optic nerve paravascular spaces from the subarachnoid space. Many proteins and peptides found in the CSF have molecular weights within the size range shown to enter the optic nerve. Of the 10 most abundant CSF proteins, eight have molecular weights less than 70 kDa.[3] These include biologically active molecules such as lipocalin-like prostaglandin D synthase (L-PGDS; β-trace), an enzyme responsible for the production of prostaglandin D_2 (PGD_2).[20] PGD_2 receptors are expressed in brain astrocytes and mediate neuroprotection.[21] Interestingly, elevated L-PGDS levels in orbital CSF are observed in pathologic optic nerve compartment syndrome seen in idiopathic intracranial hypertension[22] and normal tension glaucoma.[8] In this condition, there appears to be obstruction of CSF flow between the intracranial and optic nerve subarachnoid compartments, with ensuing protein imbalances.[22] The relevance of CSF proteins in optic nerve health and disease remains unclear, and additional studies on interactions of CSF solutes with various cell types of the optic nerve are warranted.

Entry of CSF into the optic nerve may share similarities with the recently described glymphatic system of the brain. This system consists of para-arterial influx of CSF into the brain parenchyma and paravenous clearance of interstitial fluid and solutes.[14] With the single time point assessed in this study, differential entry and exit routes for CSF and interstitial fluids could not be evaluated. Differences in vascular anatomy in the optic nerve compared to the brain also bring into question whether a glymphatic system exists in the optic nerve. The mouse retrolaminar optic nerve is invested only with capillaries invaginating from the pia mater,[17] while the brain has large penetrating arteries with thick walls surrounded by both a pial sheath and the glia limitans.[23] Whether CSF flow through the optic nerve along paravascular pathways is by simple diffusion, or a combination of diffusion and pulsatile flow of CSF associated with vascular pulsations, is unknown.

AQP4 is an integral membrane protein found on astrocytic endfeet that conducts water across cell membranes. AQP4 appears to play a role in the brain's glymphatic system.[14] In the optic nerve, astrocytic endfeet are positive for AQP4.[24] In our study, we show that AQP4-positive astrocytic endfeet border the paravascular spaces in the optic nerve. AQP4 may play a role in facilitating CSF movement into the nerve; however, future studies exploring the functional role of AQP4 in optic nerve paravascular flow are needed. Neuromyelitis optica (NMO) is a demyelinating optic neuropathy linked to the production of anti-AQP4 antibodies.[25,26] Given that AQP4 is known to facilitate bulk flow of CSF and interstitial fluids along paravascular pathways in the brain,[14] NMO optic nerve pathology may be associated with antibody-mediated obstruction of paravascular flow.

It has recently been postulated that glaucoma, a neurodegenerative disease of the visual pathway and a leading cause of blindness worldwide,[27] may be a result of an imbalance between production and clearance of neurotoxins in the optic nerve.[19,28] Accumulation of amyloid precursor protein and amyloid-β in the optic nerve is seen in mouse models of glaucoma.[29,30] We found paravascular CSF entry into the optic nerve up to and including the glia lamina, the mouse equivalent of the human lamina cribrosa. Entry of CSF tracers into the optic nerve head was not observed in our study. CSF flow through the nerve may, therefore, play a role in neurotoxin clearance in the laminar and retrolaminar optic nerve. It is unclear whether misregulation of CSF flow or glial water and solute transport in the optic nerve contributes to the pathogenesis of glaucoma. Although a few studies show changes in AQP4 expression in the optic nerve in acute IOP elevation[31] and optic nerve crush injury models,[32] further investigation of these processes in experimental glaucoma is needed.

Lastly, it would be valuable to investigate CSF/interstitial fluid and solute outflow from the optic nerve using CSF tracer injection studies with time-course analysis, or direct injection of tracer into the optic nerve. Assessing time points beyond 1 hour may also clarify whether larger molecules (>70 kDa) would eventually diffuse into the optic nerve paravascular spaces. Future studies using tracers of smaller size may also help to elucidate movement of molecules from the paravascular spaces into optic nerve parenchyma.

Conclusions

This study provides evidence of a glymphatic pathway in the optic nerve in which CSF enters the optic nerve through spaces immediately surrounding blood vessels, and these channels are bordered by AQP4-positive astrocytic endfeet. Furthermore, CSF flow into the optic nerve appears to be size-dependent. The finding of a direct communication between the CSF and tissue of the optic nerve is relevant to a fundamental understanding of optic nerve function in health and diseases, including glaucoma and other optic neuropathies.

Acknowledgments

Supported by Canadian Institutes of Health Research (MOP119432) (YHY, NG), Glaucoma Research Society of Canada (NG, YHY), Canada Foundation for Innovation #31326 (YHY, NG), the Dorothy Pitts Chair (NG), Thor and Nicky Eaton Research Fund (NG), Henry Farrugia Research Fund (YHY), National Science and Engineering Research Council CGS Award (EM), and Vision Science Research Program Award (EM).

Disclosure: **E. Mathieu**, None; **N. Gupta**, None; **A. Ahari**, None; **X. Zhou**, None; **J. Hanna**, None; **Y.H. Yücel**, None

References

1. Kapoor KG, Katz SE, Grzybowski DM, Lubow M. Cerebrospinal fluid outflow: an evolving perspective. *Brain Res Bull*. 2008;77:327–334.
2. Tsakiri A, Ravanidis S, Lagoudaki R, et al. Neuroprotective and anti-inflammatory mechanisms are activated early in optic neuritis. *Acta Neurol Scand*. 2015;131:305–312.
3. Thompson EJ. Chapter 3: The roster of CSF proteins. In: *Proteins of the Cerebrospinal Fluid - Analysis and Interpretation in the Diagnosis and Treatment of Neurological Disease*. 2nd ed. Oxford: Academic Press; 2005:13–31.
4. Zougman A, Pilch B, Podtelejnikov A, et al. Integrated analysis of the cerebrospinal fluid peptidome and proteome. *J Proteome Res*. 2008;7:386–399.
5. Berdahl JP, Allingham RR, Johnson DH. Cerebrospinal fluid pressure is decreased in primary open-angle glaucoma. *Ophthalmology*. 2008;115:763–768.
6. Ren R, Jonas JB, Tian G, et al. Cerebrospinal fluid pressure in glaucoma: a prospective study. *Ophthalmology*. 2010;117:259–266.

7. Zhang Z, Liu D, Jonas JB, et al. Axonal transport in the rat optic nerve following short-term reduction in cerebrospinal fluid pressure or elevation in intraocular pressure. *Invest Ophthalmol Vis Sci*. 2015;56:4257–4266.
8. Killer HE, Miller NR, Flammer J, et al. Cerebrospinal fluid exchange in the optic nerve in normal-tension glaucoma. *Br J Ophthalmol*. 2012;96:544–548.
9. Wostyn P, De Groot V, Van Dam D, et al. Glaucoma and the role of cerebrospinal fluid dynamics. *Invest Ophthalmol Vis Sci*. 2015;56:6630–6631.
10. Hayreh SS. Optic disc edema in raised intracranial pressure. V. Pathogenesis. *Arch Ophthalmol*. 1977;95:1553–1565.
11. Rodriguez-Peralta LA. Hematic and fluid barriers in the optic nerve. *J Comp Neurol*. 1966;126:109–121.
12. Tsukahara I, Yamashita H. An electron microscopic study on the blood-optic nerve and fluid-optic nerve barrier. *Graefes Arch Klin Exp Ophthalmol*. 1975;196:239–246.
13. Rennels ML, Gregory TF, Blaumanis OR, Fujimoto K, Grady PA. Evidence for a "paravascular" fluid circulation in the mammalian central nervous system, provided by the rapid distribution of tracer protein throughout the brain from the subarachnoid space. *Brain Res*. 1985;326:47–63.
14. Iliff JJ, Wang M, Liao Y, et al. A paravascular pathway facilitates CSF flow through the brain parenchyma and the clearance of interstitial solutes, including amyloid beta. *Sci Transl Med*. 2012;4: 147ra111.
15. Oshio K, Watanabe H, Song Y, Verkman AS, Manley GT. Reduced cerebrospinal fluid production and intracranial pressure in mice lacking choroid plexus water channel aquaporin-1. *FASEB J*. 2005;19:76–78.
16. Johnston M, Zakharov A, Papaiconomou C, Salmasi G, Armstrong D. Evidence of connections between cerebrospinal fluid and nasal lymphatic vessels in humans, non-human primates and other mammalian species. *Cerebrospinal Fluid Res*. 2004;1:2.
17. May CA, Lutjen-Drecoll E. Morphology of the murine optic nerve. *Invest Ophthalmol Vis Sci*. 2002;43:2206–2212.
18. Mathieu E, Gupta N, Macdonald RL, Ai J, Yucel YH. In vivo imaging of lymphatic drainage of cerebrospinal fluid in mouse. *Fluids Barriers CNS*. 2013;10:35.
19. Wostyn P, Killer HE, De Deyn PP. Glymphatic stasis at the site of the lamina cribrosa as a potential mechanism underlying open-angle glaucoma. *Clin Exp Ophthalmol*. 2017;45:539–547.
20. Urade Y, Hayaishi O. Prostaglandin D synthase: structure and function. *Vitam Horm*. 2000;58:89–120.
21. Liang X, Wu L, Hand T, Andreasson K. Prostaglandin D2 mediates neuronal protection via the DP1 receptor. *J Neurochem*. 2005;92:477–486.
22. Killer HE, Jaggi GP, Flammer J, Miller NR, Huber AR. The optic nerve: a new window into cerebrospinal fluid composition? *Brain*. 2006;129:1027–1030.
23. Brinker T, Stopa E, Morrison J, Klinge P. A new look at cerebrospinal fluid circulation. *Fluids Barriers CNS*. 2014;11: 10.
24. Nagelhus EA, Veruki ML, Torp R, et al. Aquaporin-4 water channel protein in the rat retina and optic nerve: polarized expression in Muller cells and fibrous astrocytes. *J Neurosci*. 1998;18:2506–2519.
25. Ratelade J, Verkman AS. Neuromyelitis optica: aquaporin-4 based pathogenesis mechanisms and new therapies. *Int J Biochem Cell Biol*. 2012;44:1519–1530.
26. Yang X, Ransom BR, Ma JF. The role of AQP4 in neuromyelitis optica: more answers, more questions. *J Neuroimmunol*. 2016;298:63–70.
27. Tham YC, Li X, Wong TY, et al. Global prevalence of glaucoma and projections of glaucoma burden through 2040: a systematic review and meta-analysis. *Ophthalmology*. 2014; 121:2081–2090.
28. Wostyn P, De Groot V, Van Dam D, et al. Glaucoma considered as an imbalance between production and clearance of neurotoxins. *Invest Ophthalmol Vis Sci*. 2014;55:5351–5352.
29. Goldblum D, Kipfer-Kauer A, Sarra GM, Wolf S, Frueh BE. Distribution of amyloid precursor protein and amyloid-beta immunoreactivity in DBA/2J glaucomatous mouse retinas. *Invest Ophthalmol Vis Sci*. 2007;48:5085–5090.
30. Kipfer-Kauer A, McKinnon SJ, Frueh BE, Goldblum D. Distribution of amyloid precursor protein and amyloid-beta in ocular hypertensive C57BL/6 mouse eyes. *Curr Eye Res*. 2010;35:828–834.
31. Dibas A, Yang MH, He S, Bobich J, Yorio T. Changes in ocular aquaporin-4 (AQP4) expression following retinal injury. *Mol Vis*. 2008;14:1770–1783.
32. Suzuki H, Oku H, Horie T, et al. Changes in expression of aquaporin-4 and aquaporin-9 in optic nerve after crushing in rats. *PLoS One*. 2014;9:e114694.

Investigative Ophthalmology & Visual Science